뇌기능 영상을 위한 TRFGE, CGE 기법에서 이미징 모드와 기울임 각의 변화에 따른 자화율 효과의 해석

정순철*, 노용만**,조장희*
*한국과학 기술원 전기및 전자공학과 **대전대학교 컴퓨터 공학과

Analysis of Susceptibility Effects by Variation of Imaging Modes and Tilting Angles in TRFGE and CGE Sequences for fMRI

S.C. Chung*, Y.M. Ro**, Z.H. Cho*
*Department of Electrical Engineering, KAIST, Seoul
**Department of Computer Engineering, Taejon University, Taejon

ABSTRACT

fMRI, functional MRI introduced recently appears based on the gradient echo technique which is sensitive to the field inhomogeneity developed due to the local susceptibility changes of blood oxygenation and deoxygenation. Common to all the gradient echo techniques is that the signal due to the susceptibility effects is generally decreased with increasing inhomogeneity due to the $T2^*$ effect or conventionally known as blood oxygenation level dependent (BOLD) effect. It is, also found that the BOLD sensitivity is also dependent on the imaging modes, namely whether the imaging is in axial, or coronal or sagittal mode as well as the directions of the vessels against the main magnetic field. We have, therefore, launched a systematic study of imaging mode dependent signal change or BOLD sensitivity as well as the signal changes due to the tilting angle of the imaging planes. Study has been made for both TRFGE sequence and CGE sequence to compare the distinctions of the each mode since each technique has different sensitivity against susceptibility effect. Method of computation and both the computer simulations and their corresponding experimental results are presented.

INTRODUCTION

Functional MRI based on the susceptibility effect and deoxygenated blood relies on the gradient echo imaging or similar techniques (1-3), such as the tailored RF gradient echo technique which we termed as TRFGE technique (4-6).

Questions raised in CGE as well as TRFGE techniques in fMRI are, however, the generality of the methods in quantitative assessment of the susceptibility effect or susceptibility difference as a function of parameters involved in the techniques, such as the echo times, repetition times, flip angles, and thickness of the slice selected and angles of the imaging slices or vessels against the main static magnetic field, B_0 as well as the imaging modes, whether the imaging mode is axial, coronal, or sagittal. Especially the latters, i.e., the angle of imaging slices, or vessels in relation to the imaging mode are closely related to the signal strength resulting from the susceptibility effect that could be developed in the imaging sequence. It is, therefore, important to investigate accurately how those slice tilting angle of the imaging slices as well as the vessels against main field affect the sensitivity of the measurements. In this paper, both experiments and computer simulations are carried out for various forms of vessels raging from a single cylinder to a bundle of capillaries tilted against main field at three different imaging modes (axial, coronal and sagittal). To observe the effects on fMRI application, both CGE and TRFGE sequences are studied and compared the results, and attempted to analyze quantitatively the susceptibility effects on fMRI.

THEORY

1. Magnetic fields and susceptibility effect

To study the distortion of the main magnetic field from the susceptibility difference between interior and exterior of a blood vessels of different sizes, a cylinder (or

capillary) is placed at the middle of a large tube filled with water and tilted to the main field. The magnetic field can be calculated from magnetic potential equation which is a Laplacian equation given in Eq. [1].

$$\frac{1}{r}\frac{\partial}{\partial r}(r\frac{\partial V}{\partial r})+\frac{1}{r^2}\frac{\partial^2 V}{\partial \varphi^2}+\frac{\partial^2 V}{\partial y^2}=0, \qquad [1]$$

where r, y, and φ are the standard cylindrical coordinates and angles, and $V(r,\varphi, y)$ is the magnetic potential, respectively. Using the method of separation of variables, the magnetic potential, $V(r, \varphi, y)$ can be written as,

$$V(r,\varphi,y) = R(r)\Phi(\varphi)Y(y), \qquad [2]$$

where $R(r)$ is function of variable r, $\Phi(\varphi)$ is function of φ and $Y(y)$ is function of y, respectively. By replacing V in Eq. [1] with Eq. [2] and with some calculations, following results are obtained,

$$\Phi(\varphi) = A_\varphi \cos\varphi + B_\varphi \sin\varphi, \qquad [3]$$

$$\frac{1}{rR(r)}\frac{dR}{dr}-\frac{1}{R(r)}\frac{d^2R}{dr^2}-\frac{1}{r^2}=m^2, \text{ and } \frac{1}{Y(y)}\frac{\partial^2 Y}{\partial y^2}=-m^2.$$

where A_φ and B_φ are the coefficients which can be evaluated from the boundary conditions. From Eq. [3], the transverse and vertical components of the main field can be obtained separately. In Fig. 1, three views, namely axial, coronal and sagittal imaging planes or views are shown with a tilt angle θ. The cylinder is a simple tube or a bundle consists of vessels or small capillaries. For each imaging mode, tilt angle is varied between 0° to 90° and measured magnetizations at all points on each plane, namely axial(xy), coronal(zx), and sagittal(yz), and calculated B_x', B_y' and B_z'.
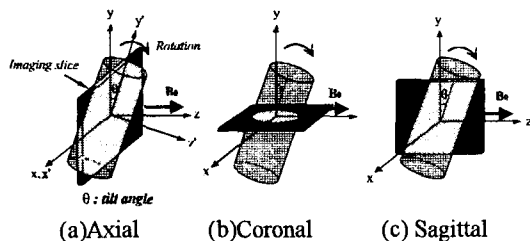

θ : tilt angle

(a)Axial   (b)Coronal   (c) Sagittal

Fig. 1 Three different imaging modes or views of a cylinder which is a simple tube or a bundle of vessels or small capillaries with an angle θ against the main magnetic field (namely axial, coronal and sagittal)

2.Application of TRFGE to the distorted magnetic fields

The TRFGE basically can add any phases on the field developed on a voxel which has a linear phase gradient developed due to the susceptibility in the thickness direction. The signal obtained may be expressed as

$$S = \left|2\pi M z_0 \ sinc\left(\frac{P_{sus}}{2\pi}z_0\right) * F^{-1}[exp[i\theta_{RF}(z)]]\right|, [4]$$

where F^{-1} represents the 1D inverse Fourier transform operator, and $*$ represents the convolution operator. This result indicates that the signal intensity given as a function of the strength of the susceptibility-induced phase gradient can be altered by an externally applied tailored RF pulse to a desired total phase distribution, i.e., altering the spin phase distribution within a voxel so that it could result in either an enhanced signal or a further attenuated signal.

EXPERIMENTAL RESULTS AND COMPUTER SIMULATIONS

Computer simulations and experiments are carried out for a single cylinder as well as bundles of capillaries with different capillary sizes. The cylinder or bundles then varied the tilting angle against the main field, B_0 for the axial, coronal and sagittal imagings or views, respectively (see Fig. 1). For the single cylinder experiments, a cylinder of diameter of $1mm$, $5mm$ and $10mm$, respectively is used. The cylinder is filled with diluted Gd_DTPA solution ($10mM$). Imaging parameters are TR/TE = $40/25msec$, flip angle $\alpha=16°$ and slice thickness=$5mm$ for both CGE and TRFGE sequences. Normalized signal intensity changes are observed with varying the tilting angle for three different imaging modes were simulated and results shown in Fig. 2(a), (b), and (c) and its corresponding experimental counterparts are also shown in Fig. 3(a), (b), and (c), respectively. These images are obtained by both with single cylinder for CGE and TRFGE sequences. Fig. 4 is the normalized signal intensity changes as a function of the tilting angle θ for sagittal views for both simulated and experimental data are shown for comparison. Although there is some differences between the simulations and experiments, the trends of variation appear same for two cases. The signal intensity changes a more or less opposite as expected for CGE and TRFGE. When the cylinder is perpendicular to the main field the susceptibility effect is maximized. Therefore, the signal intensity of the TRFGE sequence is maximized. When the cylinder gradually tilted, the susceptibility effect is also gradually decreased. The experimental results, however, show relative advantage of the TRFGE, having relatively large signal intensity over the tilt angles.
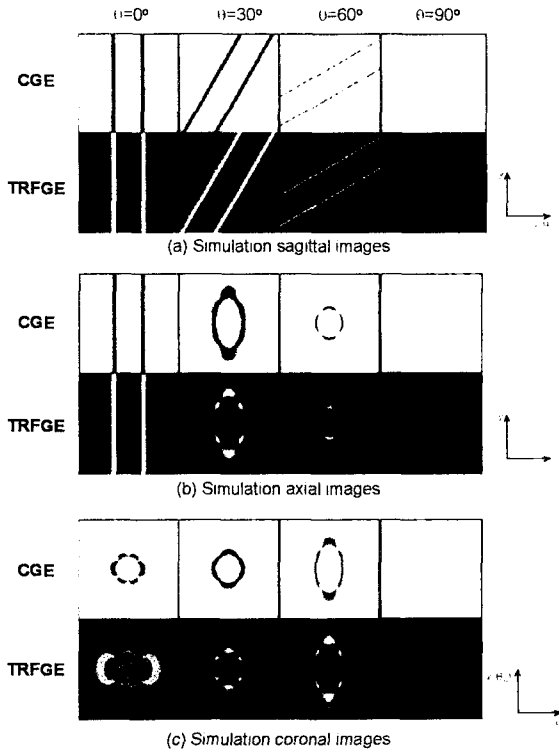
(a) Simulation sagittal images

(b) Simulation axial images

(c) Simulation coronal images

Fig. 2 Simulation images of a single cylinder with the CGE and TRFGE sequences, respectively for four tilting angles.

(a) Experimental sagittal images

(b) Experimental axial images

(c) Experimental coronal images

Fig. 3 Experimental images of a single cylinder with the CGE and TRFGE sequences, respectively for four tilting angles.

More crucial and mimicking the true situation is experiments with small capillary tube bundles. For the capillary bundle experiments, a $15mm$ diameter bundle consists of 40 pieces of $1mm$ diameter tubes and $10mm$ diameter bundle with 200 pieces of $300\mu m$ diameter tubes lumped together are used (see Fig. 5). The experimental phantom also consists of two capillary bundles of two different susceptibility values, namely $20mM$ and $18mM$ Gd_DTPA solutions, respectively, as shown in Fig. 5. The resulting susceptibility difference indicates a corresponding value of $0.05ppm$. Imaging parameters were TR/TE=$40/25msec$, flip angle $\alpha=30°$ and slice thickness =$10mm$. Fig. 6 show experimental data of sagittal images obtained from the $15mm$ and $10mm$ diameter bundles with the CGE and TRFGE sequences, respectively for the two Gd_DTPA solutions ($18mM$ and$20mM$) with varying the tilting angles.
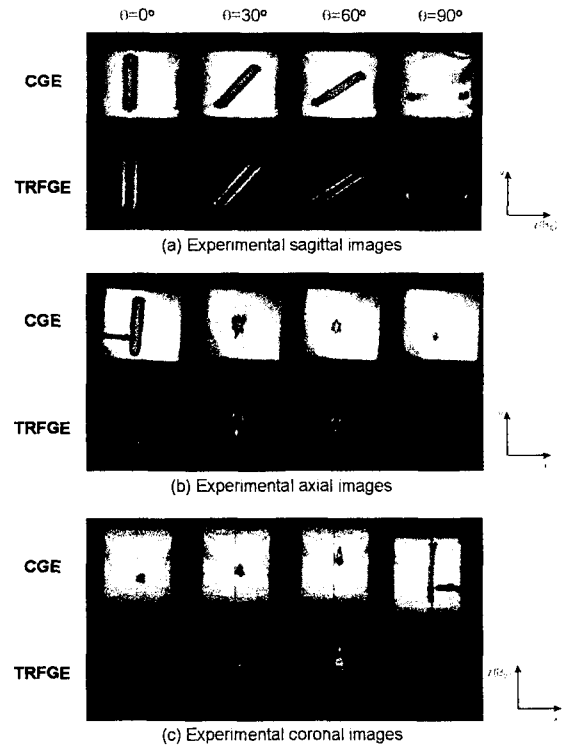
CGE sequence ——
TRFGE sequence

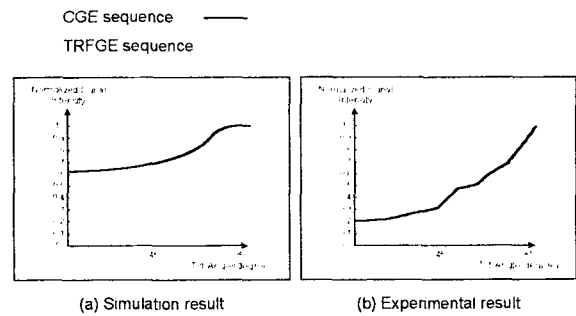(a) Simulation result   (b) Experimental result

Fig. 4 Normalized signal changes as a function of the tilting angle for sagittal views with the CGE and TRFGE sequences, respectively. (a) Simulation result (b) Experimental result
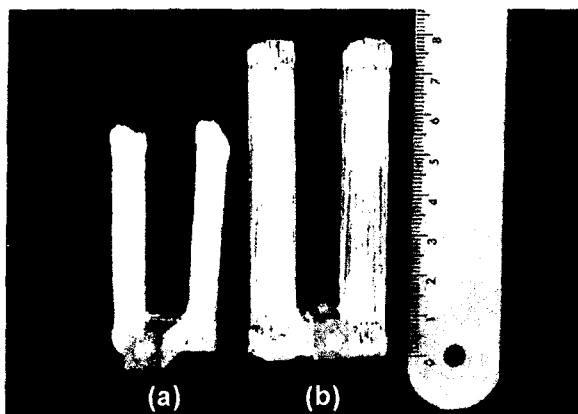
Fig. 5 For the capillary experiments, a 15mm diameter bundle consists of 1mm diameter tubes and 10mm diameter bundle with 300μm diameter tubes lumped together are used. Also two capillary bundles with two different susceptibility values, namely 20mM and 18mM Gd_DTPA solutions are used to measure the contrast sensitivity. (a) 10mm diameter bundles, each with 200 pieces of 300μm diameter tube. (b) 15mm diameter bundles, each with 40 pices of 1mm diametertube.
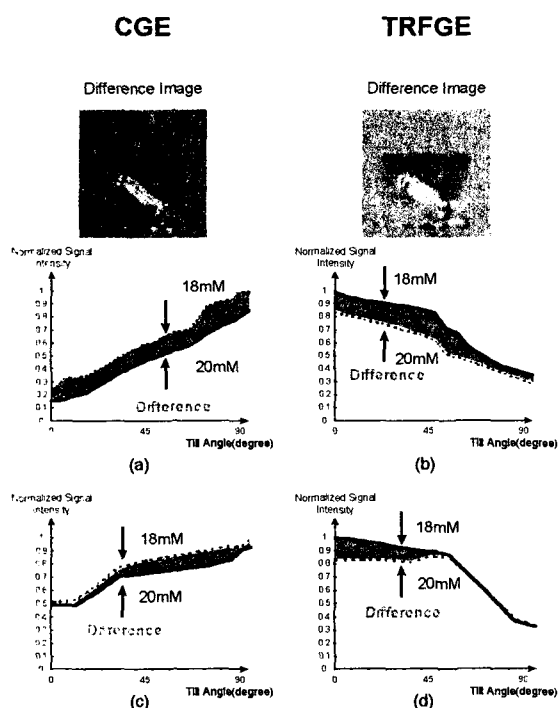

Fig. 6 The normalized signal intensity curves obtained from 15mm and 10mm diameter tube bundles with varying the tilting angles against the main magnetic field for the two Gd_DTPA solutions (18mM and 20mM). Data obtained from the CGE sequence (a & c). Data obtained from the TRFGE sequence (b & d).

Fig. 6(a) and (b) show the signal intensity changes and difference of the set in the 15mm diameter bundles as a function of the tilting angle for the CGE and TRFGE, respectively. Signal intensity changes in the 10mm diameter bundles as a function of the tilting angle are also shown in Fig. 6(c) and (d) for the two Gd_DTPA solutions. Although there are some differences between the large capillaries (1mm tubes) and small capillaries (300μm tubes) bundles, the trend of signal intensity variation appears same for the two cases. The signal intensity as well as the differences has the tendency of decreasing with increasing tilting angle for the TRFGE sequence while for the CGE the trends were opposite.

CONCLUSION AND DISCUSSION

For the quantitative understanding of the "BOLD" effect, it was necessary to examine various factors, namely imaging modes (sagittal, axial, coronal), assumptions of vessel layouts (line tilt angles of the vessels and capillaries or bundle of the capillaries), and also the pulse sequences employed. It was found that the maximum "BOLD" sensitivity seems obtainable with the spatial imaging. For the parallel capillary bundles of two different sizes clearly show the difference in intensities as a function of tilt angles (see Fig. 6(a) and (b)). The differences, however, was relatively insensitive to the tilt angles. Two examples of gradient echo sequences (CGE and TRFGE) show similar difference sensitivities (20mM to 18mM) with an opposite trend, however, TRFGE appears less sensitive to the tilt angle showing relatively constant differences till $\theta=60°$. Present study also suggested that the pulse sequence such as the TRFGE sequence clearly superior to the conventional BOLD sensitive techniques such as the conventional gradient echo (CGE) sequence, the later (TRFGE) not only shows superior contrast sensitivity over CGE but also insensitive to inflow effect as well as bulk susceptibility effect which undesirable information of measuring the capillaries and distinguishing the capillaries from that of the large venous vessels.

REFERENCES

1. K.K.Kwong et al, Proc. Natl, Acad. Sci. (USA), 89, 5675-5679, 1992.
2. S.Ogawa et al, Proc. Natl, Acad. Sci. (USA), 87, 9868-9872, 1990.
3. R.Tunner et al, Magn. Reson. Med. 29, 277-279, 1993.
4. Z.H.Cho et al, in Proc., SMR, 659, 1994.
5. Z.H.Cho et al, Int. J. Imag. Sys. Tech, 6, 164-170, 1995.
6. Z.H.Cho et al, Magn. Res. Med. 35, 1-5, 1996.